General Disclaimer

One or more of the Following Statements may affect this Document

- This document has been reproduced from the best copy furnished by the organizational source. It is being released in the interest of making available as much information as possible.

- This document may contain data, which exceeds the sheet parameters. It was furnished in this condition by the organizational source and is the best copy available.

- This document may contain tone-on-tone or color graphs, charts and/or pictures, which have been reproduced in black and white.

- This document is paginated as submitted by the original source.

- Portions of this document are not fully legible due to the historical nature of some of the material. However, it is the best reproduction available from the original submission.

Produced by the NASA Center for Aerospace Information (CASI)

(NASA-CR-169435) STUDY OF THE PHOTOVOLTAIC EFFECT IN THIN FILM BARIUM TITANATE Semiannual Report (New Mexico Univ.) 23 p HC A02/MF A01 CSCL 10A
N83-10567
Unclas
G3/44 38320

THE UNIVERSITY OF NEW MEXICO
COLLEGE OF ENGINEERING

OCT 1982
RECEIVED
NASA STI FACILITY
ACCESS DEPT.

BUREAU OF ENGINEERING RESEARCH

STUDY OF THE PHOTOVOLTAIC EFFECT IN THIN FILM BARIUM TITANATE

by

W. W. Grannemann
and
Vineet S. Dharmadhikari

Semi-Annual Report No. EECE-274(82) NASA-931-1
Work Performed under NASA Contract No. NAG 1-95

October 1982

STUDY OF THE PHOTOVOLTAIC EFFECT IN THIN FILM BARIUM TITANATE

by

W. W. Granneman

and

Vineet S. Dharmadhikari

Work Performed Under
NASA Contract No. NAG 1-95

October 1982

TABLE OF CONTENTS

1. Introduction

This report presents results on the basic mechanism associated with the photovoltaic phenomena observed in the R.F. sputtered $BaTiO_3$/silicon system. Series of measurements of short-circuit photocurrents and open-circuit photovoltage were made. Furthermore, we have also investigated the composition-depth profiles and the interface characteristics of the $BaTiO_3$/silicon system for a better understanding of the electronic properties. These results were obtained with the help of a Scanning Auger Microprobe combined with ion in-depth profiling.

2. Experimental

The details of the film and device processing are described at length in the previous reports [1, 2]. Briefly, the $BaTiO_3$ were sputtered onto single crystal n and p type silicon wafers from a 5-inch diameter 99.99% pure $BaTiO_3$ target. Before the film deposition, the wafers were thoroughly cleaned following the standard procedures for cleaning silicon for FET's.

The composition-depth profiles were obtained with the help of a Physical Electronics Industries (PHI) Model 590 Scanning Auger System. The vacuum system was degassed until a base pressure of about 10^{-10} torr was reached. The primary beam energy E_p was 5.0 keV permitting the beam size to be reduced to 0.2 μm by electrostatic focusing. The AES data were recorded in the usual first derivative mode $\left[\frac{dN(E)}{dE}\right]$ using 4V peak-to-peak modulation and 1 msec time constant (RC). The depth profiles were recorded by sputtering with 3 kV argon ions, and an ion gun emission current up to 25 mA was used.

3. Results and Discussion

3.1 Photovoltaic properties

When a device is illuminated with near-UV light without any applied field, at least three important physical effects can take place [3].

1. Photoexcitation of carriers both from the trapping centers in the $BaTiO_3$ band gap and across the band gap by near-UV light of energy equal to or greater than the band gap.

2. Carriers photoexcited to the conduction state diffuse (with no field applied) or drift under the influence of an applied field to new trapping sites beyond the absorption depth of the $BaTiO_3$. Retrapped carriers establish a space charge field E_{SC} which modulates the applied field E_A and aids in the domain switching process.

3. A transient photocurrent I_{SC} is associated with the photoexcited carriers which are retrapped to establish E_{SC}. Carriers remaining in the conduction state contribute to a steady-state photovoltaic current I_{PV}, which is driven by the bulk photovoltaic effect [4]. The photocurrents I_{SC} and I_{PV} both exist in the domain nucleation and thus help the domain switching process.

Since poled ferroelectric $BaTiO_3$ is also pyroelectric, therefore, in addition to the effects enumerated above, photon absorption produces a temperature rise which results in a transient pyroelectric current I_{PY}.

If the device is short-circuited and one of the surfaces of $BaTiO_3$ is illuminated with near-UV light, all components of the photocurrent I_{hv} are proportional to the light intensity I. This effect is illustrated in Figure 1 which shows I_{hv} plotted

as a function of time. The curve shows the transient I_{py} and steady-state I_{pv} for the light-on condition and the transient I_{py} for the light-off condition. From about 20 to 35 seconds, the curves represent the steady-state I_{pv}. The steady-state I_{pv} is proportional to the absorbed light intensity, I.

$$I_{pv} = K\alpha I \tag{1}$$

where I is the intensity and K is a constant depending on the nature of the absorption center and the host lattice. This is illustrated in the inset of Figure 2.

The open-circuit photovoltage V_{oc} as a function of time is plotted in Figure 2 for two devices. The transient voltages from 0 to 15 seconds are due to a transient pyroelectric charge V_{py}. From about 15 to 40 seconds, at which time the light is turned off, V_{oc} is a constant independent of intensity, I. When the light is turned off, the transient voltage V_{py} decays to zero with the dielectric relaxation time of the material.

Under open-circuit conditions, the photocurrent charges the $BaTiO_3$ capacitance generating a macroscopic electric field E_i given by

$$J = K\alpha I + \sigma E_i \tag{2}$$

where σ is the electrical conductivity of the $BaTiO_3$ film during illumination, so that in the steady state, the saturation field

$$E_{sat} = \frac{K\alpha I}{\sigma} \tag{3}$$

Open-circuit saturation voltages (V_{oc}) corresponding to fields of about 24 KV/cm are observed in $BaTiO_3$ films [2, 5]. For intensities greater than 7 mW/cm^2, the open-circuit saturation field is independent (Figure 3) as expected from Equation 3. Further, we also observed the photovoltage to increase as the

poling voltage was increased, until the polarization saturated. However, the magnitude of the photovoltage in the two directions of the polarization was quite different. This difference may probably be due to the presence of an intermediate layer.

Figure 4 shows a family of 60 Hz hysteresis loops obtained from a $BaTiO_3$ device [2, 5]. The figure indicates that saturation polarization was not attained with the field amplitude applied since the polarization continued to increase with increasing sinusoidal switching field. This effect results from the specific properties of the silicon/sputtered $BaTiO_3$ film. Between the silicon and the sputtered ferroelectric film, an intermediate layer with a markedly distorted crystal lattice exists. The strong domain fixing in this intermediate layer, which has a high concentration of defects, hinders the switching process. With an increase in the amplitude of the switching field, the number of domains switching also increases causing an increase in the maximum value of P determined from the experimental hysteresis loop. Further, the presence of an intermediate layer has been established from the layer-by-layer analysis of the Auger spectra of the ferroelectric $BaTiO_3$/silicon system. The results obtained from such studies are presented in the following section.

3.2 Auger Analysis

Auger spectra for the $BaTiO_3$ films deposited on silicon substrates at different deposition temperatures in the energy range between 0 and 2000 eV are shown in Figure 5. Figure 5(a) shows the spectrum taken at the surface of the film deposited on n-Si substrate held at room temperature. Figure 5(b) is for film deposited on n-Si at 580°C, while Figure 5(c) is a spectrum taken for film deposited on p-Si at 583°C. As can be observed, apart from the main elements (Ba, Ti, and O) the surface contains

traces of carbon and sulphur impurities. Also note the carbon spectrum in Figure 5(a) is different as compared to the carbon spectrum in Figures 5(b) and 5(c). The carbon signal probably results from the adsorption of carbon containing atmospheric gases. Another source lies in hydrogen molecules forming part of the vacuum oils of the system in which the films were sputtered. The sulphur impurity may have been left after the standard cleaning procedure used in the device processing. However, the changes in the shape of the carbon spectrum in Figure 5(a) as compared to Figures 5(b) and 5(c) indicate the formation of a carbon compound with a different type of chemical bond.

By recording peak-to-peak height as a function of removal of material by ion sputtering, the information about the depthdistribution of the chemical elements in the sample can be obtained [6]. The chemical depth profiles of oxygen KLL, titanium LMM and barium MNN through the $BaTiO_3$/silicon structures as a function of ion sputtering time are shown in Figures 6-8. The parameters are similar to those of Figures 5(a)-(c), respectively. The cross section of the films contains three regions, an external surface layer, a main layer, and an intermediate film-substrate layer. The external surface contains an excess of barium. Apart from this, the surface layer has a considerable amount of adsorbed carbon, and hence oxygen combined with the latter. This aspect, as well as the deficit of Ti, causes an increase in the proportion of oxygen on the surface.

After the removal of the surface layer the concentration curves (i.e., in the main layer) exhibit plateaus, the extent of which is a function of deposition temperature. For films synthesized at room temperature, an excess of Ti, relative to films formed at high substrate temperature is observed.

The chemical depth profiles of the intermediate layer indicate that the $BaTiO_3$ interfaces are not abrupt but form a

continuous region of varying chemical composition. More detailed analysis of the interface region shows the formation of titanium dioxide $TiO_{2-x}(x < 2)$. The analysis also shows that $SiO_x(x < 2)$ is formed. Another interesting feature observed is that the width of the intermediate layers, with other parameters constant, is a function of deposition temperature. The width of the intermediate layers is more for films formed at higher substrate temperature. Two possibilities can be considered: (i) the diffusion of Ba, Ti, and O into the substrate, and (ii) the out-diffusion of silicon into the sputtered film. During the sputter deposition, electron and ion bombardment of the substrate occurs leading not only to heating but also to creation of point defects at the surface. Figure 9 shows the spectrum taken after the $BaTiO_3$ film was sputtered out. Presence of Ti, Ba, and O is still observed. Of these the concentration of titanium is high. The presence of argon is due to argon atoms implanted during the sputtering process and is not an inherent impurity in the $BaTiO_3$.

Thus, experimentally, the formation of the following types of layers in R.F. sputtered $BaTiO_3$ films on silicon are observed:

1. an external surface layer containing carbon and an excess of barium up to several tens of angstroms thick,
2. the main layer with stable composition, but the concentration is dependent on the evaporation condition, and
3. an intermediate film-substrate layer consisting of the components $TiO_{2-x}(x < 2)$, and the interdiffusion of Ba, Ti, O, and Si. The formation of the TiO_{2-x} layer is due to the combination of high temperature and vacuum, which favors the reducing process. The adhesion

coefficient of oxygen falls rapidly with increasing temperature which shifts the equilibrium of the reaction $BaTiO_3 = BaO + TiO_2$ to the right. On the other hand, the volatile BaO reevaporates with greater probability than TiO_2.

Therefore, the films of complex composition are layered systems in which the surface external layer differs in composition from the main layer. Intermediate film-substrate layers are also formed, consisting of variable composition oxide. These layers are not ferroelectric or else they hinder the switching process. Such layers, together with the defects in the main layer dilute the ferroelectric phase. The effect of this is seen on certain ferroelectric parameters, such as shift in Curie point, broadening of the ε-T curve, lowering of remanent polarization and dielectric constant, increase in coercive field and also the dielectric losses.

Jona and Shirane [7] have discussed the nature of surface layers of ferroelectrics and classified them on the basis of two models--space change layers due to ion vacancies, and layers formed by chemical or mechanical action which takes no part in the polarization reversal process, but will give rise to interface charges. Our experimental results are in favor of the second model.

4. CONCLUSIONS

The results on open-circuit and short-circuit measurements illustrate the role of the photovoltaic field, photovoltaic current and the photoconductance in photoferroelectric domain switching. The results also illustrate the pyroelectric properties of the devices and, in general, provide an important basis for the better understanding of the observed phenomena.

Auger electron spectroscopy has been successfully used in conjunction with argon-ion sputtering to determine the chemical nature of MFS structures and to measure the quantity and distribution of barium, titanium, and oxygen in the bulk $BaTiO_3$ films. It was observed that the $BaTiO_3$/silicon interface was not abrupt but forms a continuous region of varying chemical composition. We feel that it is this intermediate layer and the surface external layer that are formed which dilute or degrade the ferroelectric properties of the MFS devices.

ACKNOWLEDGMENT

The research has been supported by the National Aeronautics and Space Administration (NASA) under Contract No. NAG-1-95. The authors deeply appreciate the help extended by the Air Force Weapons Laboratory, Kirtland Air Force Base, New Mexico in performing the Auger measurements.

REFERENCE

1. Granneman, W. W. and Dharmadhikari, V. S., UNM (semi-annual) Technical Report, No. EE-268 (81) NASA-931-1.
2. Grannemann, W. W. and Dharmadhikari, V. S., UNM (annual) Technical Report No. EE-273 (82) NASA-931-1.
3. Land, C. E., and Percy, P. S., Ferroelectrics, 27, 1980, 131.
4. Glass, A. M., Von der Linde, D., and Negran, T. J., Journal of Elecronic Materials, 4, 1975, 915.
5. Dharmadhikari, V. S. and Grannemann, W. W., Journal of Applied Physics, Manuscript No. R-2821.
6. Holloway, P. H., and Stein, H. J., Journal Electrochemical Society, 123, 1976, 723.
7. Jona, F. P., and Shirane, G., Ferroelectric Crystals, Pergamon, New York, 1962.

LIST OF FIGURES

ORIGINAL PAGE IS
OF POOR QUALITY

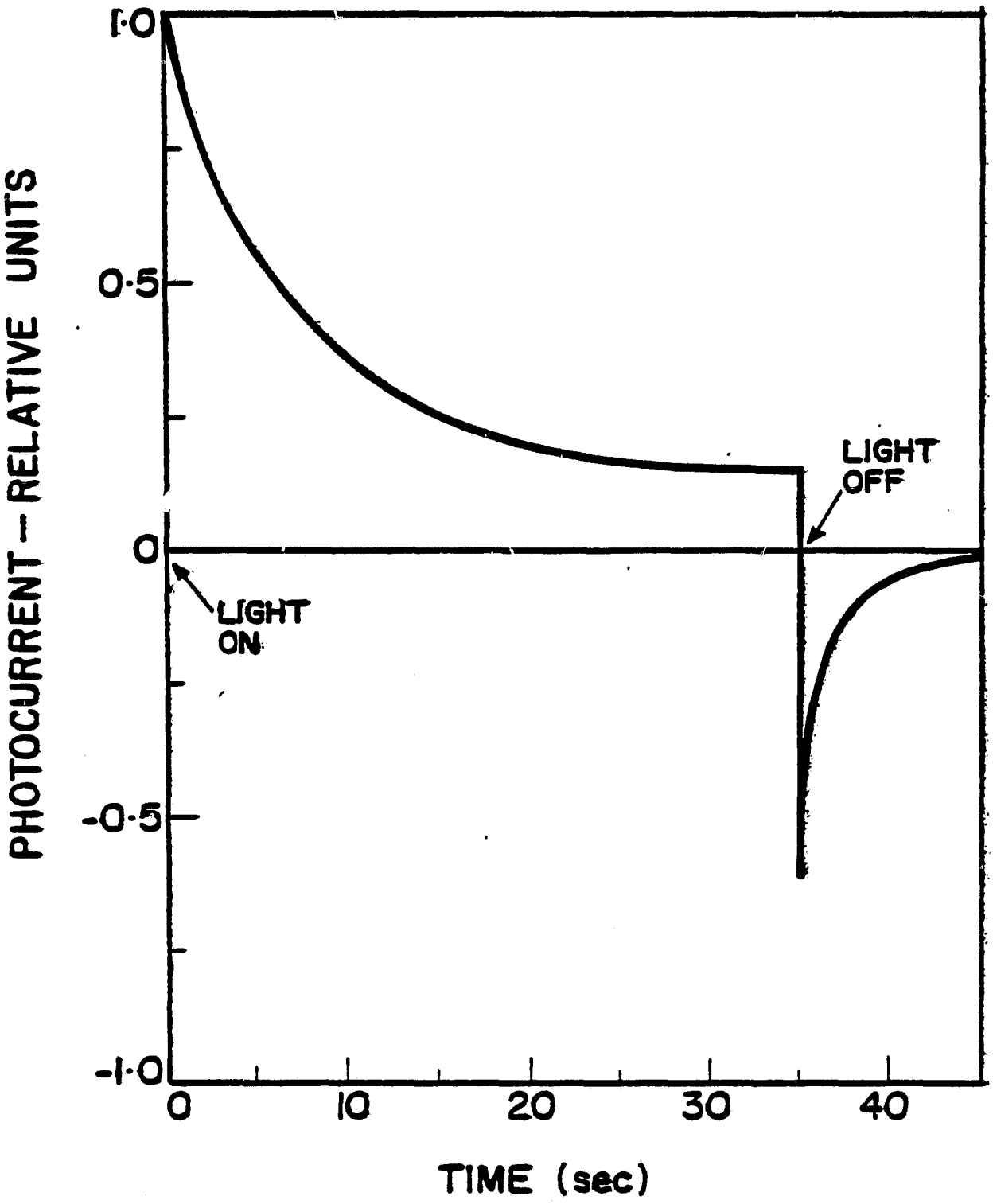

Figure 1. Short-circuit photocurrent in $BaTiO_3$ thin film as a function of time.

ORIGINAL PAGE IS
OF POOR QUALITY

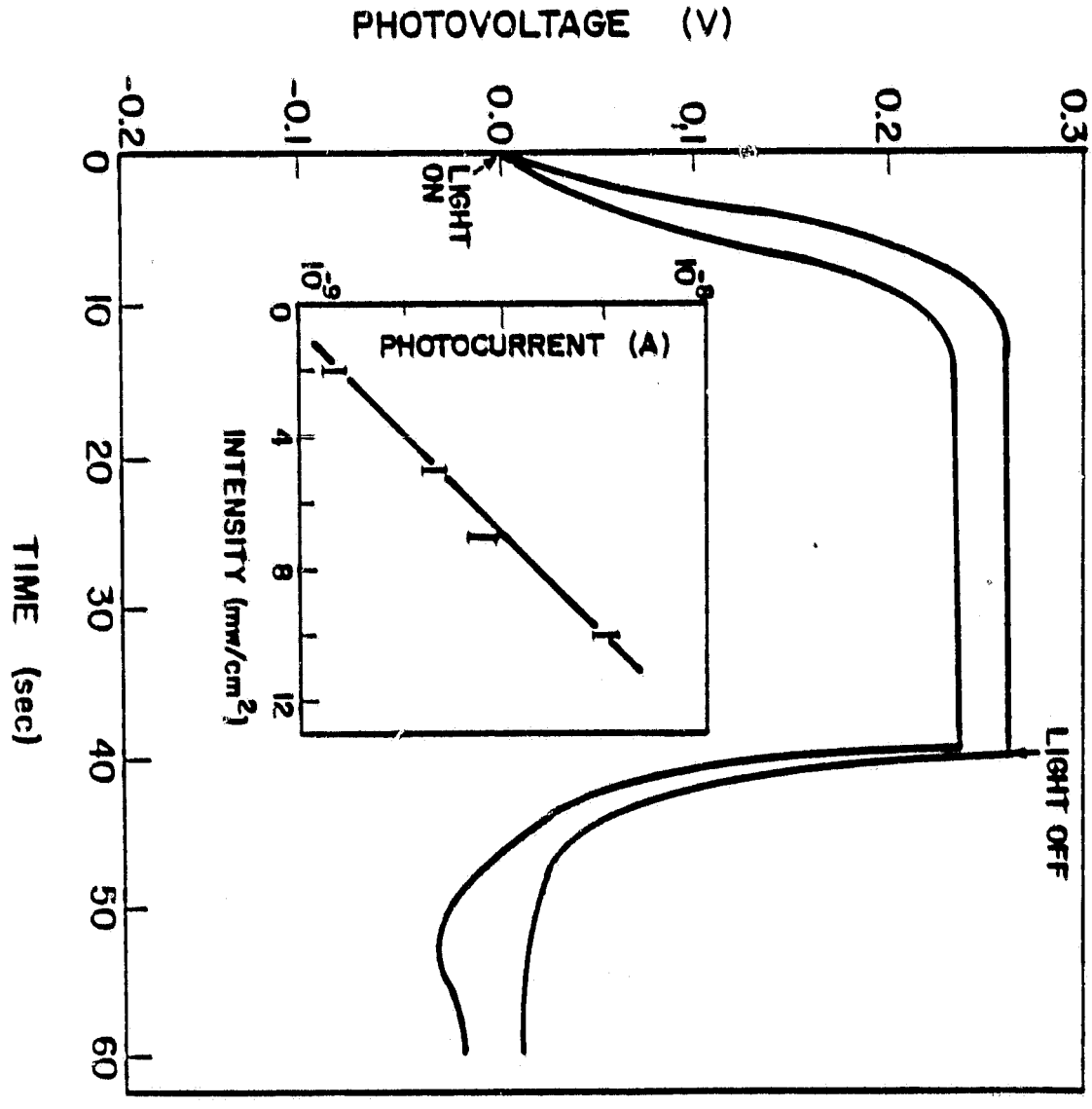

Figure 2. Open-circuit photovoltage as a function of time for two different $BaTiO_3$ film devices. The inset shows the photocurrent (I_{pv}) versus light intensity.

ORIGINAL PAGE IS
OF POOR QUALITY

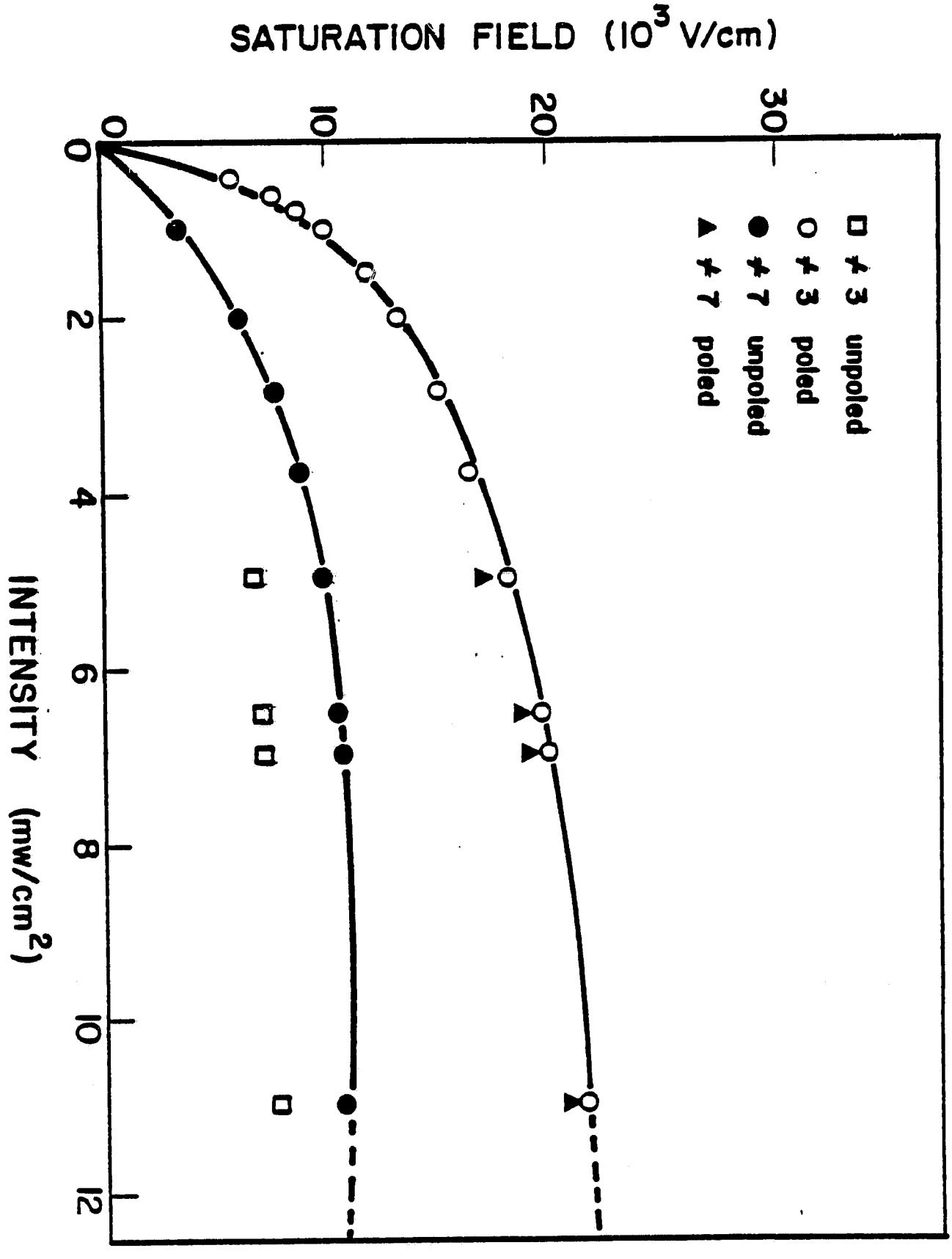

Figure 3. Open-circuit saturation field as a function of intensity of illumination for two devices under poled and unpoled conditions.

ORIGINAL PAGE IS
OF POOR QUALITY

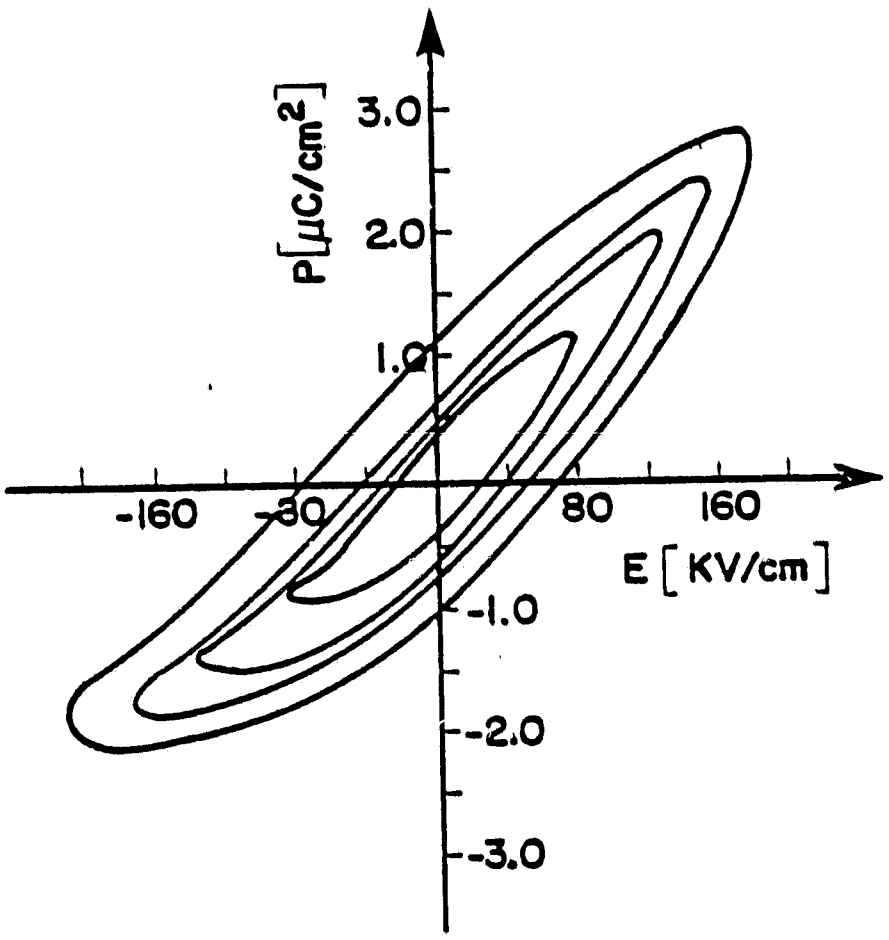

Figure 4. P-E hysteresis loops for 60 Hz sine wave at four amplitudes of 3.9, 6, 8, and 14 V.

ORIGINAL PAGE IS
OF POOR QUALITY

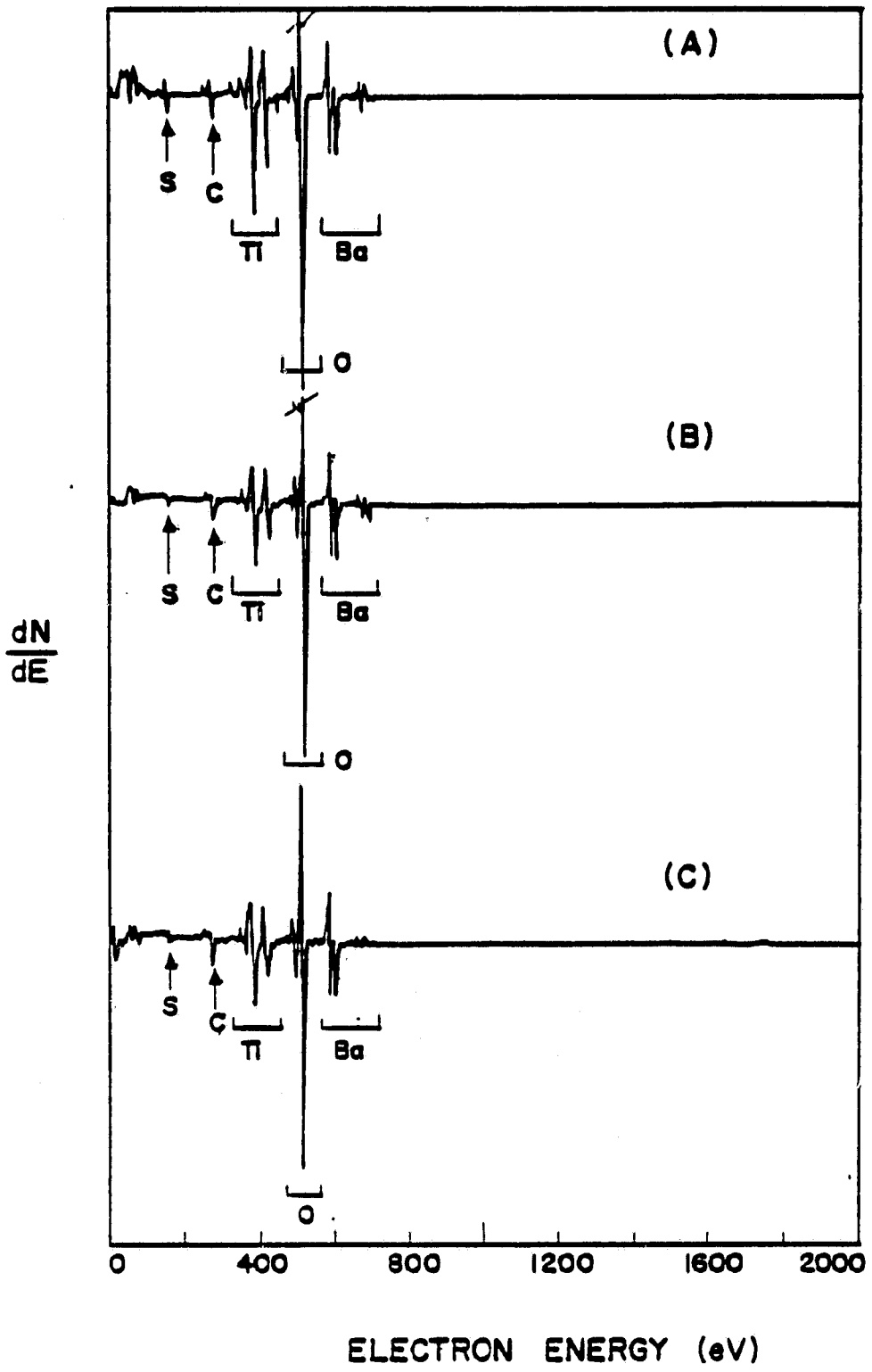

Figure 5. Auger survey spectrum from the surface of $BaTiO_3$ film sputtered on silicon substrate (a) n-Si; 55°C, (b) n-Si; 580°C, and (c) p-Si; 583° C.

ORIGINAL PAGE IS
OF POOR QUALITY

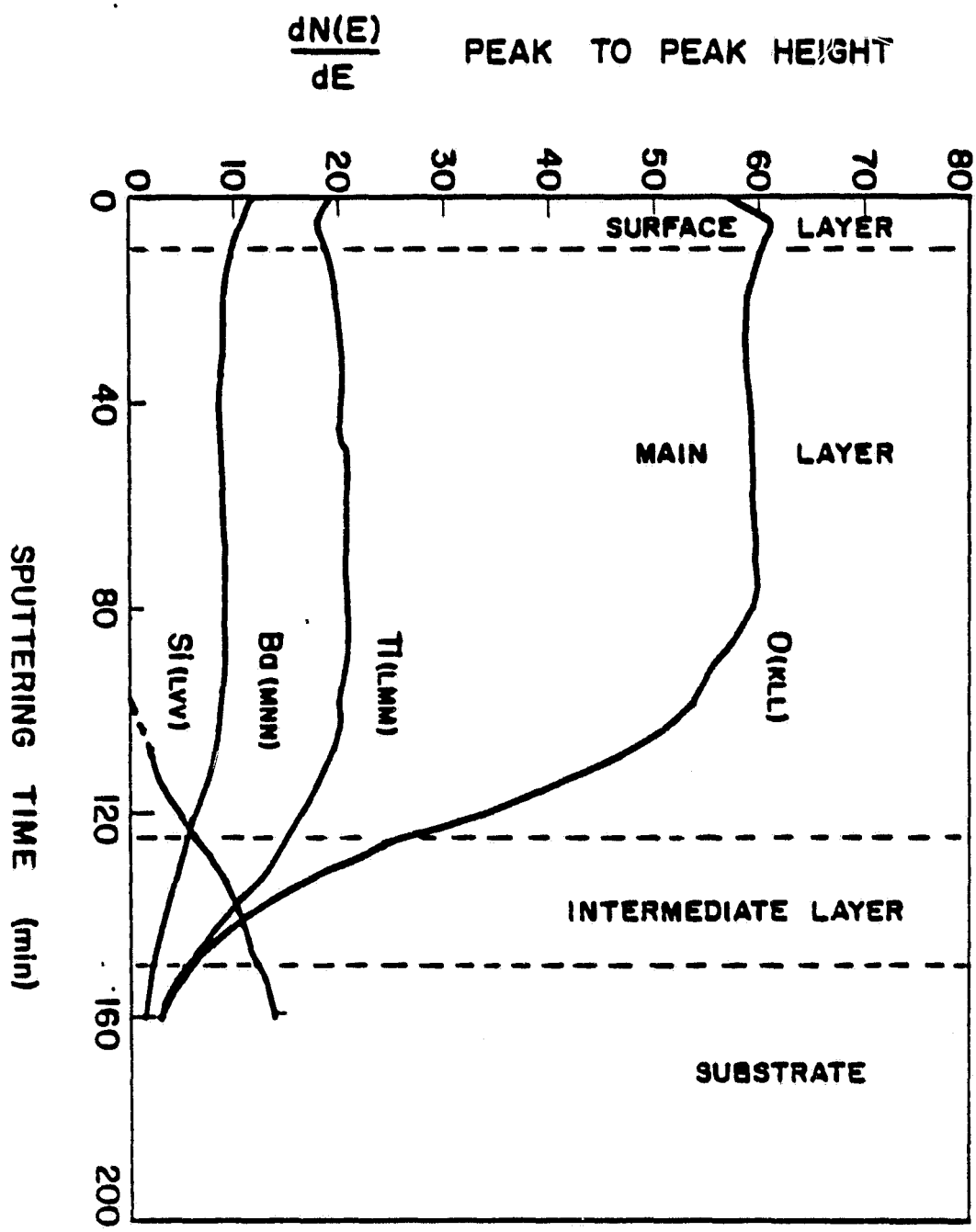

Figure 6. Derivative Auger depth profile through $BaTiO_3$ films sputtered on n-silicon (substrate temperature = 55°C; Ar/O_2 ratio = 95.5; deposition rate = 7 Å/min).

ORIGINAL PAGE IS
OF POOR QUALITY

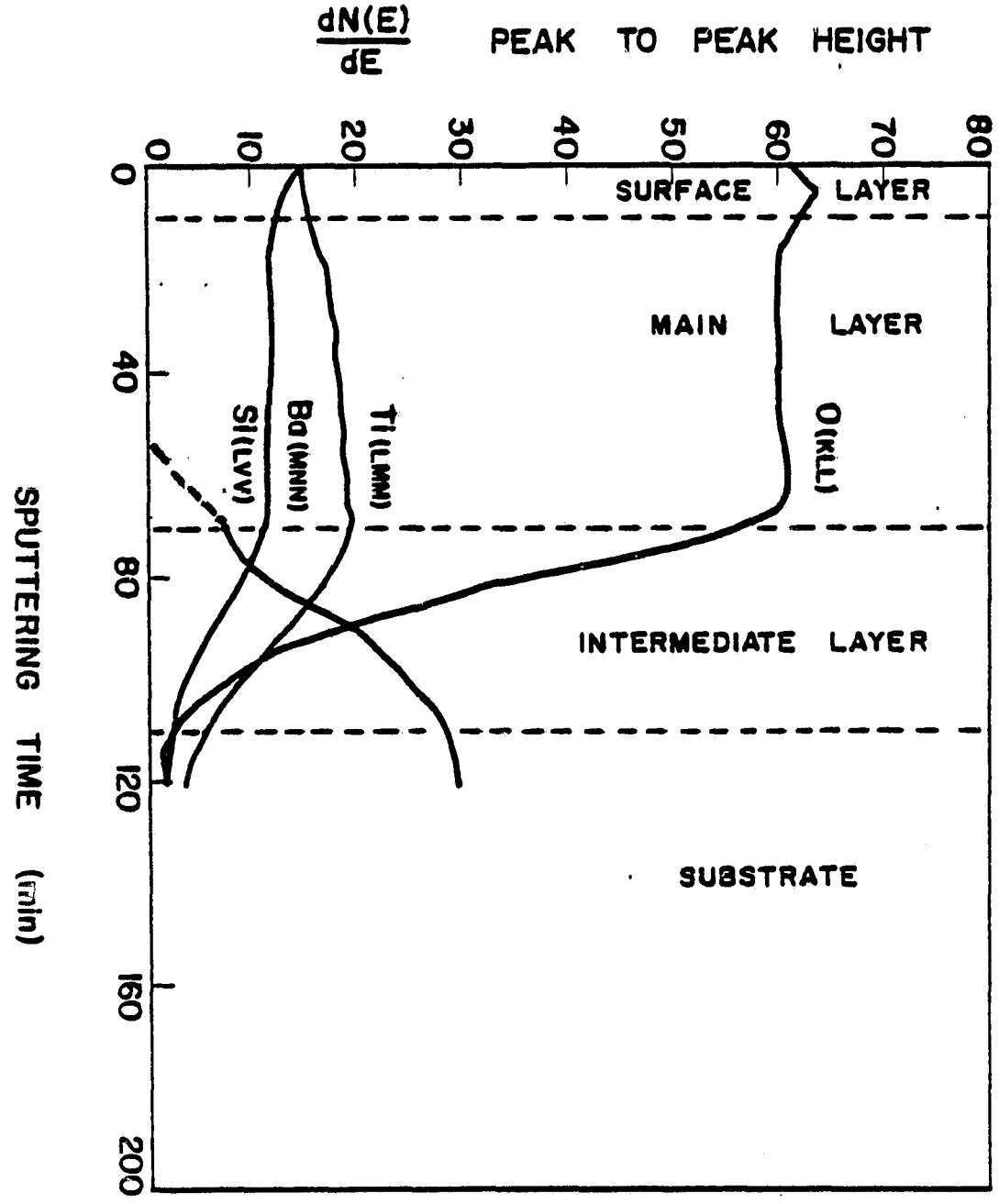

Figure 7. Derivative Auger depth profile through $BaTiO_3$ films sputtered on n-Si (substrate temperature = 580°C; Ar/O_2 ratio = 95.5; deposition rate = 5 Å/min).

ORIGINAL PAGE IS
OF POOR QUALITY

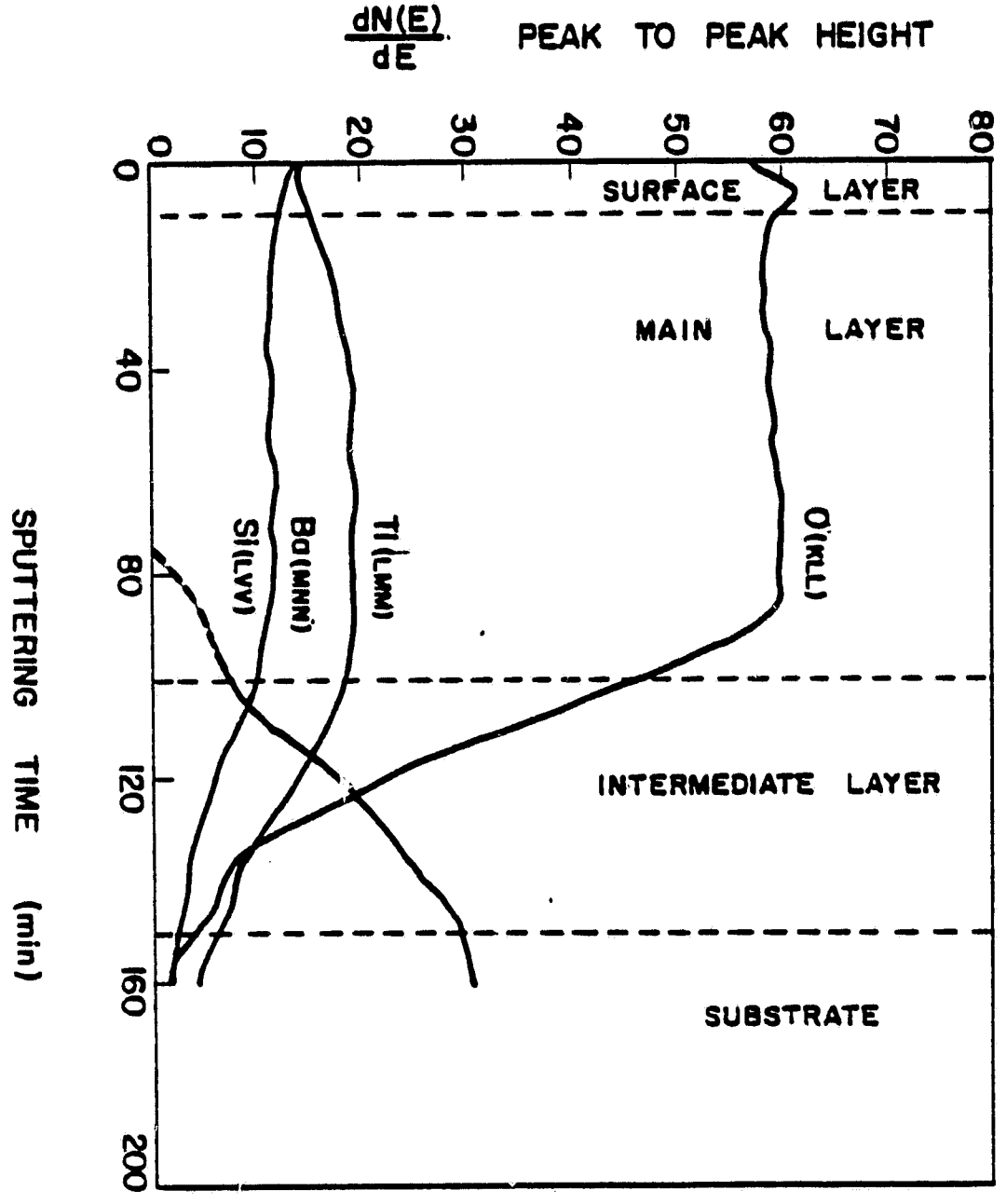

Figure 8. Derivative Auger depth profile through $BaTiO_3$ films sputtered on p-Si (substrate temperature = 583°C; Ar/O_2 ratio = 95.5, deposition rate = 6 Å/min).

ORIGINAL PAGE IS
OF POOR QUALITY

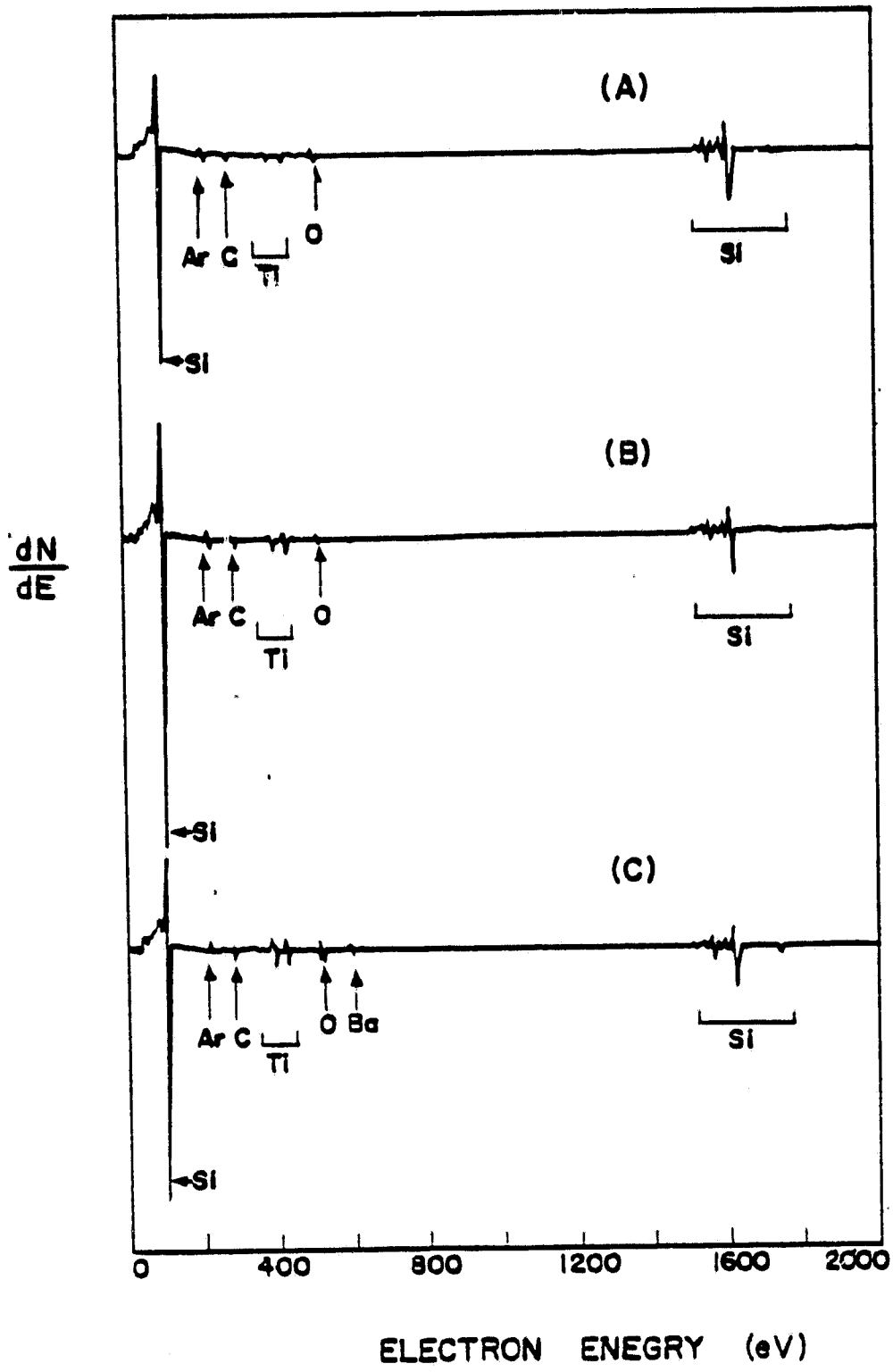

Figure 9. Typical Auger survey spectrum from the $BaTiO_3$/silicon interface after the $BaTiO_3$ film is sputtered out (parameters same as Figures 6-8, respectively).